Calcif Tissue Int (2007) 81:394–402
DOI 10.1007/s00223-007-9077-2

Particle-Induced Osteolysis in Three-Dimensional Micro-Computed Tomography

Christian Wedemeyer · Jie Xu · Carl Neuerburg · Stefan Landgraeber · Nasser M. Malyar · Fabian von Knoch · Georg Gosheger · Marius von Knoch · Franz Löer · Guido Saxler

Received: 4 July 2007 / Accepted: 7 September 2007 / Published online: 21 October 2007

Abstract Small-animal models are useful for the in vivo study of particle-induced osteolysis, the most frequent cause of aseptic loosening after total joint replacement. Microstructural changes associated with particle-induced osteolysis have been extensively explored using two-dimensional (2D) techniques. However, relatively little is known regarding the 3D dynamic microstructure of particle-induced osteolysis. Therefore, we tested micro-computed tomography (micro-CT) as a novel tool for 3D analysis of wear debris-mediated osteolysis in a small-animal model of particle-induced osteolysis. The murine calvarial model based on polyethylene particles was utilized in 14 C57BL/J6 mice randomly divided into two groups. Group 1 received sham surgery, and group 2 was treated with polyethylene particles. We performed 3D micro-CT analysis and histological assessment. Various bone morphometric parameters were assessed. Regression was used to examine the relation between the results achieved by the two methods. Micro-CT analysis provides a fully automated means to quantify bone destruction in a mouse model of particle-induced osteolysis. This method revealed that the osteolytic lesions in calvaria in the experimental group were affected irregularly compared to the rather even distribution of osteolysis in the control group. This is an observation which would have been missed if histomorphometric analysis only had been performed, leading to false assessment of the actual situation. These irregularities seen by micro-CT analysis provide new insight into individual bone changes which might otherwise be overlooked by histological analysis and can be used as baseline information on which future studies can be designed.

Keywords Micro-computed tomography · Histomorphometry · Osteolysis · Polyethylene particle · Mouse

C. Wedemeyer (✉) · C. Neuerburg · S. Landgraeber · M. von Knoch · F. Löer · G. Saxler
Department of Orthopedics, University of Duisburg-Essen, Hufelandstr. 55, 45122 Essen, Germany
e-mail: christian.wedemeyer@uni-duisburg-essen.de

J. Xu
Department of Orthopedics, Second Affiliated Hospital of Sun Yat-sen University, Guangzhou, China

N. M. Malyar
Department of Cardiology, University of Duisburg-Essen, Hufelandstr. 55, 45122 Essen, Germany

F. von Knoch
Schulthess Clinic, Lengghalde 2, 8008 Zürich, Switzerland

G. Gosheger
Department of Orthopedics, University of Münster, Albert-Schweitzer-Str. 33, 48149 Münster, Germany

Aseptic loosening resulting from particle-induced osteolysis has been the subject of intensive research because of its catastrophic effect on the outcome of total joint replacement [1]. Particles, especially ultrahigh-molecular weight polyethylene particles (UHMWPE) emerging from shear and frictional forces, affect the surrounding tissues by reaching into the articular cavity and via phagocytosis into the newly originated capsule. Depending on the number of particles, this initiates an aseptic inflammatory response, which can be compensated for initially but subsequently leads to inflammatory destruction of the bone when the number of particles increases [2].

Several animal models have been established to examine particle-induced osteolysis. Shanbhag et al. [3] used an in vivo model of a rabbit in which they implanted a mixture

of particles consisting of polyethylene, titanium alloy, and cobalt-chromium alloy into the hip joint. The in vivo examination in the small-animal model, primarily established by Merkel et al. [4] and Schwarz et al. [5], particularly demonstrated the advantage of observing particle-induced osteolysis achieved by a brief invasive procedure over a short period of time. They used titanium particles and inhibited particle-induced osteolysis using bisphosphonates. Our group [6] altered the animal model by applying UHMWPE particles.

The large variability observed in the mechanism cannot be evaluated unless structural properties of reactive bone are included in the analysis. Histomorphometry is still a necessary source used to analyze particle-induced osteolysis and osteolysis in general within the range of the midline suture of mouse skulls in many studies [5, 7, 8]. However, histomorphometry allows only two-dimensional (2D) analysis of bone structures. Moreover, cutting a sample into thin slices distorts the intact volume and a repeated evaluation of the specimen by any other method is made very difficult, if not impossible. Micro-computed tomography (micro-CT), which has been used in research on osteoporosis, allows 3D visualization and analysis of bone structures, including assessment of bone volumetric parameters.

Based on previous studies carried out by our group [9, 10] in which we observed increased osteolysis in mouse skulls that had been treated with UHMWPE particles, this study is intended to evaluate the potential of micro-CT as a new method for assessment of particle-induced osteolyis.

Materials and Methods

Animal Model

We used a calvarial model of UHMWPE particle-induced osteolysis in 14 12-week-old C57BL/J6 male mice. The murine calvarial model was recently introduced by our group and is based on the original model of calvarial osteolysis [4, 11]. The animals were divided into two groups randomly. The animals in group 1 ($n = 7$) underwent sham surgery only, and the animals in group 2 ($n = 7$) received UHMWPE particles. The animal experiment was approved by the university's ethics committee and the local authorities according to official guidelines.

Particles

Clariant (Gersthofen, Germany) supplied the commercially pure UHMWPE particles (Ceridust VP 3610). More than 34% of the particles were smaller than 1 μm, with a mean particle size (given as equivalent circle diameter) of 1.74 ± 1.43 μm (range 0.05–11.6) [9].

For decontamination of endotoxins, particles were washed twice in 70% ethanol at room temperature for 24 hours. Testing for endotoxins using a quantitative limulus amebocyte lysate assay (Charles River, Margate, UK) at a detection level of <0.25 EU/mL was negative. The particles were washed in phosphate-buffered saline and afterward dried in a desiccator.

Surgical Procedure

Before surgery, mice were anesthetized by intraperitoneal injection. A 10-mm incision was made over the calvarial sagittal midline suture. A 1.0 x 1.0 cm area of periosteum was exposed and left intact. In sham controls (group 1) the incision was closed without any further intervention. Group 2 received 30 μL of dried polyethylene particles (2 x 10^8 particles/1,000 μL; the dosage was established through previous experiments [9]), which were distributed over the periost using a sterile sharp surgical spoon. The incision was sutured. Water and food were given ad libitum. Fourteen days after operation, the animals were killed in a CO_2 chamber as our previous research had shown that particle-induced osteolysis can be detected from this time point [12, 13].

Micro-CT

In this study, a high-resolution micro-CT (Skyscan 1072; Skyscan, Aartselaar, Belgium) was used to perform qualitative and quantitative analyses of murine calvarial bone in order to ascertain whether this method is also suitable for obtaining evidence of the degree of osteolysis in mouse skulls.

Technical Specifications of the Micro-CT

The micro-CT system is based on a scanner developed for high-resolution imaging (up to 4 μm cubic voxels) of sample sizes up to 2 cm^3. The scanner uses a field X-ray tube with an 8 μm spot size and expected lifetime of >10,000 hours. The tube operates between 20 and 100 keV with a current of up to 100 μA. For scanning, the samples are placed between the microfocus X-ray source and a charge-coupled-device (CCD) detector (matrix size 1,024 x 1,024 pixels, field of view 25 mm^2). In order to prevent the samples from moving during scanning, the plain heads are placed in a tightly fitting rigid plastic tube. In the scanner's chamber the specimens are placed in a pile on a computer-controlled precision stage,

which is rotated in equiangular steps of 0.9° around an angle of 180°. When placed between the X-ray source and the CCD detector, the cone-beam of X-rays passes the object and then hits the CCD detector, thus acquiring 2D X-ray images. A personal computer is used to control the scanner and to store the CCD image data recorded at each angle of view during the scanning process.

Tomographic Image Reconstruction

The X-ray projection data of the scanned samples are then submitted to the resident reconstruction program (Cone-beam Reconstruction, Skyscan), which is based on a Feldkamp filtered backprojection algorithm [14, 15], resulting in a volume image of up to 10,243 voxels, each cubic voxel being 4–19 μm on a side, depending on how much of the specimen had to be imaged.

Parameters of Micro-CT Analysis

For qualitative analysis, 3D images of the mice heads were then reconstructed from the cross-sectional slices using Analyze® software (version 6.0; Biomedical Imaging Resource, Mayo Clinic, Rochester, MN). In order to visually illustrate the effect of UHMWPE particle-induced osteolysis on the osseous properties of the mouse skulls, a constant fixed threshold level (the minimum threshold value at 5 and the maximum threshold value at 200) was used for rendering the 3D images of the skulls (Fig. 1).

For quantitative analysis of UHMWPE particle-induced osteolysis, a square-shaped region of interest (ROI) of approximately 2 x 2 mm with the midline suture of the skull in its center was placed in one of the 2D-reconstructed slices, as described by Perilli and Baruffaldi [16]. In the next step, 100 ROIs were combined in order to create a volume of interest of about 2 x 2 x 2 mm in size.

Then the resident quantitative analysis software (CTAn, Skyscan) was used to obtain the following parameters: bone volume (BV), bone surface (BS), and BS/BV. As osteolysis is expressed by a loss in BV, the term "osteolytic lesion" can be appropriately used rather than "decreased BV." The analysis was then repeated using the same ROI chosen for the first assessment to calculate smaller piles of 10 slices each. Finally, a reference curve was assessed using the average BV values.

Specimen Retrieval and Histological Processing

The calvaria of all animals were removed as an elliptical plate of bone defined by the foramen magnum, auditory canals, and orbits. Sections (4 μm) were taken in the frontal plane centered over the area of particle-induced osteolysis. These sections were stained with Goldner dye [4, 11]. The Goldner-stained sections were analyzed by transmission light microscopy (Axiophot, Zeiss, Germany). The existence and dimension of granulomatous foreign body reaction and bone resorption were evaluated.

Bone Histomorphometry

Using a standard high-quality light microscope, the specimens were photographed with a digital camera (Camedia C-5060 WZ; Olympus, Hamburg, Germany). A histomorphometric analysis was made by image analysis software (UTHSCA Image Tool, IT version 3.0; University of Texas, San Antonio, TX). The area of soft tissue, including any bone resorption pits in the midline suture, was traced in Goldner sections to determine the eroded surface in the midline suture [17]. Using one microscopic field at a magnification of x20, the ROIs, i.e. the nonosseous tissue areas adjacent to and in continuity with the midline suture, were encircled by the operator. For bone thickness

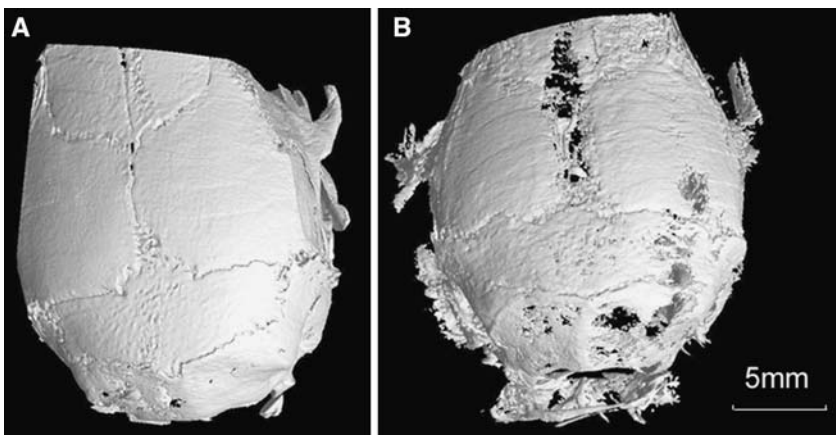

Fig. 1 Reconstruction of a C57BL/J6 mouse skull. **a** After surgery without UHMWPE particle implantation (group 1). **b** Following UHMWPE particle implantation (group 2). The 3D pictures show that the skull surface of the animal that underwent particle implantation appears more lacerated than the skull of the control mouse

measurements, the specimens were divided into four 0.5-mm steps to the left and four equivalent steps to the right side of the midline suture. Bone thickness was measured at the chosen sites and in the midline suture.

Statistical Analysis

Data are reported as mean ± standard deviation (SD). Pearson's correlation coefficient was used to assess the relationship between the 2D diameter from histological sections and the 3D diameter from micro-CT. Linear regression analysis was used to assess the linear relationship between BV and BS determined by micro-CT, both in the control group and in the experimental group. Student's *t*-test was used to analyze the difference in osteolysis between the two groups. Analysis of variance (ANOVA) was used to compare the interblock difference of bone loss in mice. Differences were considered significant at the 0.05 level.

Results

Quantitative Assessment of Total Bone Loss

One mouse in the control group did not recover from anesthesia; all the other mice tolerated the experimental procedures well. There were no problems with wound healing.

The results were obtained via micro-CT and quantitative histomorphometry, with BV as a general value obtained by micro-CT-analysis and the eroded surface of the mouse skull as a value obtained by histomorphometry and an associated image analysis system.

For the control group, the eroded surface values measured from histological sections and BV obtained via micro-CT were 0.04 ± 0.0126 mm^2 and 0.984 ± 0.0245 mm^3, respectively. For the experimental group, the eroded surface values measured from histological sections and BV obtained via micro-CT were 0.26 ± 0.0830 mm^2 and 0.842 ± 0.0682 mm^3, respectively. In an initial comparison of the values, BV was significantly larger ($P < 0.05$) in the animals that did not receive particles and the eroded surface of the control mice was significantly smaller ($P < 0.05$).

There was a strong negative correlation between the eroded surface and BV ($R^2 = 0.966$, $P < 0.01$), indicating that an enlarged eroded surface area of the midline suture is accompanied by a decrease in BV and vice versa. This observation suggested that the quantity of bone loss could be assessed by either histomorphometric or micro-CT analysis.

Spatial Distribution of Bone Loss in the Sagittal Plane Direction

Distributional micro-CT analysis was performed for a capacious cubic area within the mouse skull, consisting of 100 slices subdivided into ten smaller blocks consisting of only ten slices each. The pooled values of these blocks are illustrated in Fig. 2 for each mouse in the control group. Distribution of bone mass within the cubic area seems to be regular for each mouse in the control group. Furthermore, the mice in the control group seemed to react very similarly to each other, as demonstrated by the reference curve based on average values of BV (Fig. 3).

$$y = y_0 + a * \exp\left[-0.5 * \left(\frac{\mathrm{In}\left(\frac{x}{x_0}\right)}{b}\right)^2\right]$$

y is the BV of the cubic area; x is the number of the cubic area in the sagittal direction

$$a = 1.095 * 10^{-2},\ b = 8.31 * 10^{-1},$$
$$x_0 = 5.15,\ y_0 = 8.737 * 10^{-2}$$

In comparison, the widespread irregularity of osteolytic lesions seen in particle-treated animals makes evaluation of a reliable reference curve impossible. Therefore, the individual observations noted in animals of the experimental group are shown in Fig. 4, in which the variances of the blocks in each mouse are compared to the reference curve for the control group. The volume of bone loss of the blocks ranged from –0.00729 to 0.026390 mm^3. One-way ANOVA was used to analyze the differences in bone loss between every two blocks in the particle-treated animals. Due to the obvious irregularity in the distribution of osteolytic lesions in each mouse, an accompanying significant ($P < 0.05$) irregularity of bone loss was found (Fig. 5).

Analysis of the distribution of bone loss revealed that there was one animal in which the osteolytic lesions were evenly distributed, which contrasted with what we observed in the other animals of the experimental group. All the steps of the experimental setup were reviewed, and no abnormality was detected. This controversial observation could not be attributed to any known factors.

Linear regression analysis revealed that there was a significant linear relationship between BV and BS, both in the control group and in the experimental group ($P < 0.05$) (Fig. 6). However, the inclination of the straight lines indicating the relationship between BV and BS of the particle or the control group was different. The inclination was 31.25 in the experimental group, which is smaller than the value of 48.77 in the control group. Thus, a decrease in BS is accompanied by a decrease in BV, and this effect was

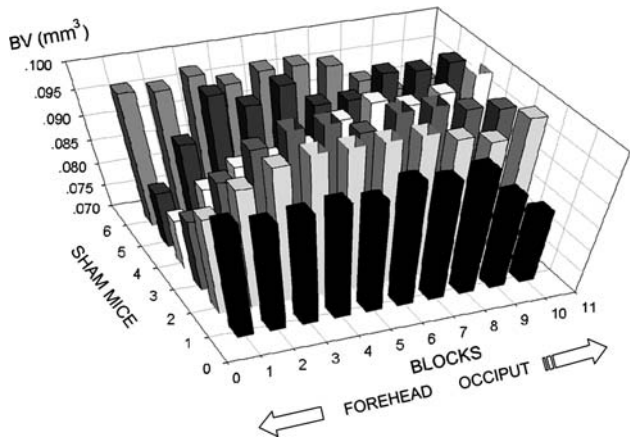

Fig. 2 Distribution of BV in the chosen ROI in the control group (group 1). Each block consisted of ten micro-CT slices

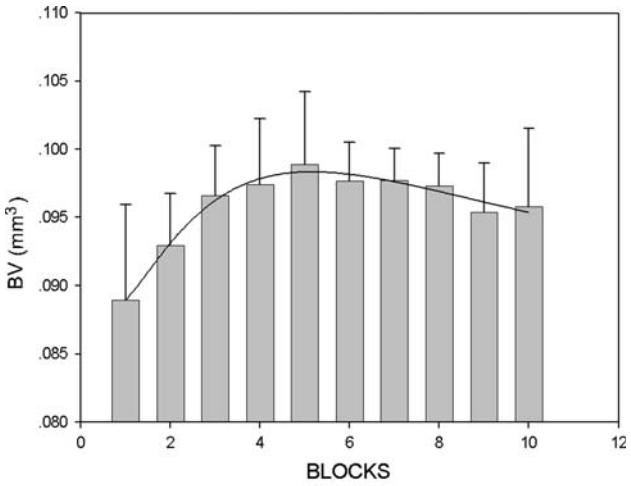

Fig. 3 Average BV evaluated for each of the ten blocks within the ROI. The reference curve illustrates the similar behavior of the bone in the control group (group 1). The formula of the curve was calculated by the data of each block of the mice in the control group

less distinctive in the particle-treated group than in the control group. In conclusion, there was more BS in the particle-treated animals associated with irregular interblock osteolysis. In other words, the higher the osteolytic variation, the bigger the interblock differences of the individual mouse. Hence, the irregularity of the osteolytic lesions induces changes in the BS.

Spatial Distribution of Bone Loss in the Coronal Plane Direction

We also investigated the distribution of osteolysis in the coronal direction. Here, we initially describe the investigations obtained by histomorphometric analysis in which the thickness of the skull was evaluated.

The thickness of the calvaria was measured histomorphometrically at different radii (0, 0.5, 1.0, 1.5, 2.0 mm), with the midline suture in its center. The difference in the thickness of the control calvaria and the particle-treated calvaria was then evaluated using two-way ANOVA. Comparison revealed that significant changes in calvarial thickness only occurred close to the midline suture (Fig. 7). There was no distinct significance at the edge of the calvarial specimens.

Micro-CT analysis of spatial distribution of osteolysis in the coronal plane revealed the following findings. Calvarial BV was also assessed at different distances from the midline suture, and two-way ANOVA was used to analyze the differences between the control and experimental groups. There was significant osteolysis in the central section of the skull but not in the parietal bone. In contrast to histomorphometric analysis, micro-CT analysis revealed a significant difference in bone loss between the particle-treated group and the control group at a distance of 1.5 mm from the midline suture (Fig. 8). These findings suggest that significant details of particle-induced bone loss may remain undetected when osteolysis is evaluated by means of histological sections with a section-to-section distance of 200 μm, as used in the present and multiple previous studies.

Discussion

Aseptic loosening is initiated by an aseptic inflammatory response to phagocytosis of implant wear particles [1]. When the prosthesis head is placed into the socket, shear and frictional forces lead to the production of numerous implant wear particles. The amount of implant wear particles exceeds the removal capacity of the lymphatic system, and extensive formation of granulation tissue occurs, leading to fibrous necrosis. When the newly created capsule starts to participate in the inflammatory response to the debris, BV progressively decreases due to osteolysis [18, 19]. If the released wear particles are distributed uniformly throughout the periprosthetic tissues, the number of particles per unit volume of tissue can be related directly to the wear volume [20]. However, because of the variation in permeability of these tissues and the limited pathways available for particle access, it is unlikely that the distribution is uniform. A local accumulation of wear particles could produce local osteolysis, even though the overall density of particles is low. Many studies [21, 22] have revealed that, in contrast to the uniform bone loss seen in osteoporosis, the quantity of bone loss varies in the different parts of the tissue surrounding prostheses. The distribution and extent of osteolysis related to the type and magnitude of wear particles seems to be a key factor in

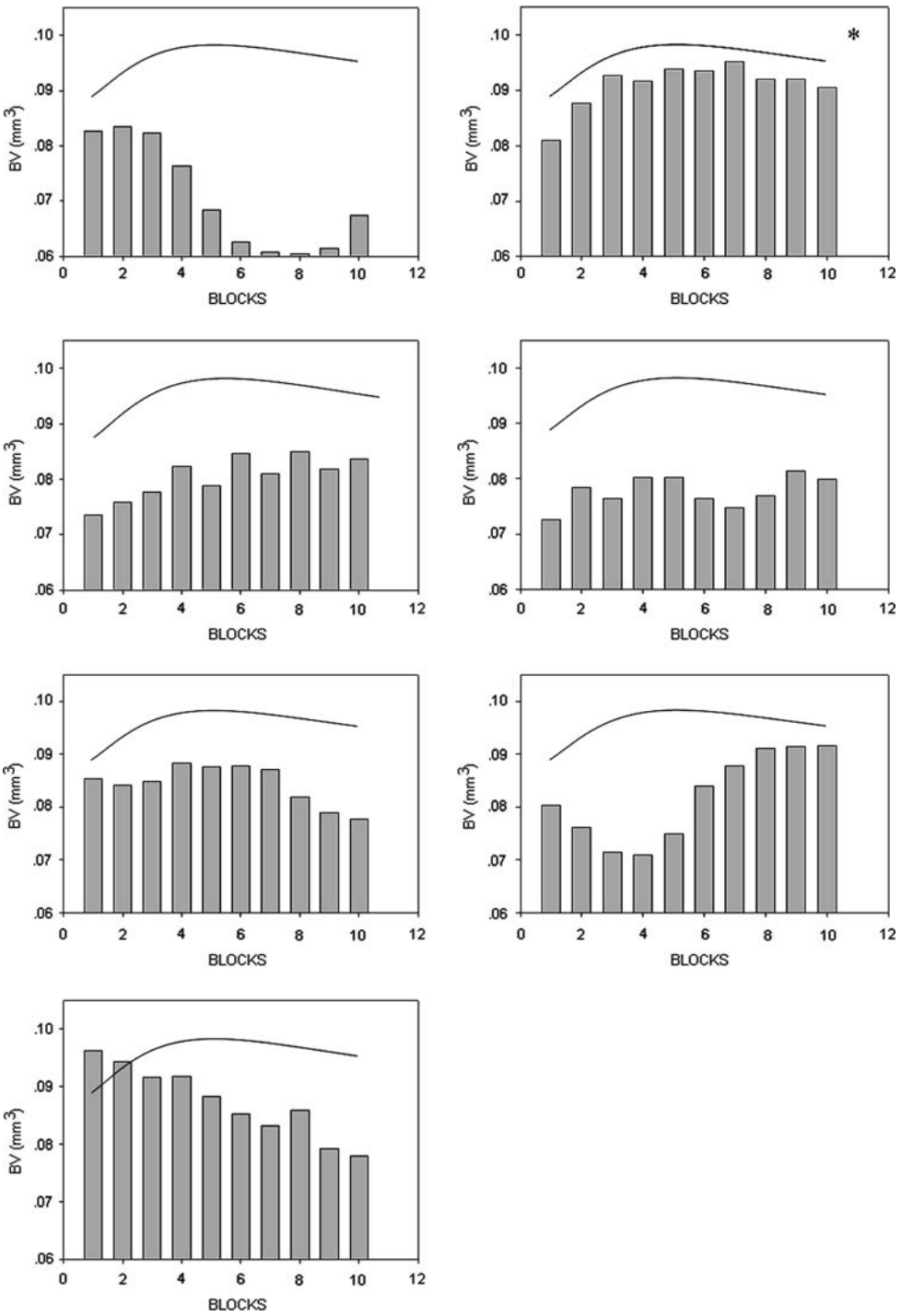

Fig. 4 Average BV assessed for each mouse in the particle-treated group (Group 2). The reference curve at the top of each histogram indicates the overall reference curve calculated for the control group (Group 1) with the exception of one animal (*). There was a significant irregular distribution of the inter-block osteolysis in the mice belonging to the experimental group (Group 2). Compared to the reference curve for the control group, the volume of osteolysis of the blocks ranged from –0.00729 mm^3 to 0.026390 mm^3

avoiding particle-induced osteolysis, and a great deal of research has focused on this issue. Pronounced osteolysis was reported in the femoral environment. As the femoral bone is shaved down using a rasp, there is only cortical bone left at the distal two-thirds of the femoral component, whereas the proximal third retains cancellous bone. Therefore, the research on particle-induced osteolysis in the femur mainly concentrates on the loss of cortical bone caused by particles emerging from the implant. Until now, many studies [23, 24] focusing on the morphology of osteoporosis have been carried out with micro-CT. However, the morphology of cortical bone differs from that in trabecular bone. Furthermore, as mentioned above, distribution of osteolysis differs from that of osteoporosis. For these reasons, the following parameters (i.e., the bone volume fraction [BV/TV], trabecular thickness [Tb.Th], trabecular separation [Tb.Sp], trabecular number [Tb.N], and degree of anisotropy [DA]) stated for trabecular bone

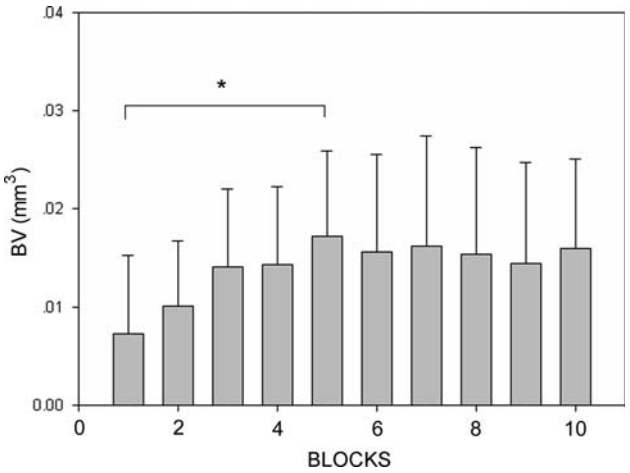

Fig. 5 Distribution of volume of bone loss in the experimental group (group 2). Bars represent mean ± SD. Statistically significant differences of bone loss between the first and the fifth blocks ($*P < 0.05$) as determined by one-way ANOVA

in previous trials [25–27] focused on osteoporosis were excluded.

Since we have not found any other studies about particle-induced osteolysis concentrating on analysis of the correlation between micro-CT technology and histomorphometry, the locations chosen for histomorphometric analysis, equivalent to the ones used in former studies, were reassessed by micro-CT analysis. Firstly, the total bone loss within the ROI was found to be significantly different as confirmed by both micro-CT and histomorphometry, and close correlation was found between the parameters from the two methods. Secondly, the analysis of interblock bone loss was based on the data revealed by micro-CT, which showed that the bone loss was irregularly distributed, as stated above. At the same time, the distribution of bone loss was also evaluated by the thickness of the calvaria using histomorphometric analysis. This revealed the unexpected finding that bone loss in the range of the parietal skull was less pronounced, as confirmed by 2D histomorphometry. However, there were significant differences when 3D micro-CT analysis was applied. We considered that our results did not negate the fact that the resolution in light microscopy is far higher (<1 μm) than that of micro-CT, which is only 20 μm. However, it was almost impossible to analyze so many sections using histomorphometry with a chosen section-to-section distance of 1 μm. The histomorphometric analysis in our, and many other, studies was based on several sections with a distance of more than 20 μm. The large distance between the sections may have lost some details because the distribution of bone loss due to osteolysis was not uniform.

This finding confirmed that micro-CT is a fast and reliable method for morphological analysis of experimental particle-induced osteolysis and could become a valuable substitute for histology. It enables construction of 3D images of either the entire specimen or only a small block within the ROI for subsequent investigations. Compared with histological sections analyzed in two dimensions with the sutures located perpendicularly to the longitudinal axis, CT images are versatile as they can be inspected in either two or three dimensions.

The animal model used in our research was introduced by Merkel et al. [4]. The particles were directly implanted in the periosteal space instead of according to the "replace the joint with implant" [28] principle. With the ready-made wear particles, the osteolysis was detected in a short time. However, the simulation of the distribution and local accumulation of wear particles in different parts around the implant was limited. In clinical research [29, 30] it was found that high wear rates may not lead to osteolysis when the implants are so well fixed to the bone that debris cannot penetrate the fixation interfaces. As shown in this study, micro-CT technology makes it possible to reveal the non-uniform bone loss linked to varied accumulation of particles in different parts; we did not expect to find new

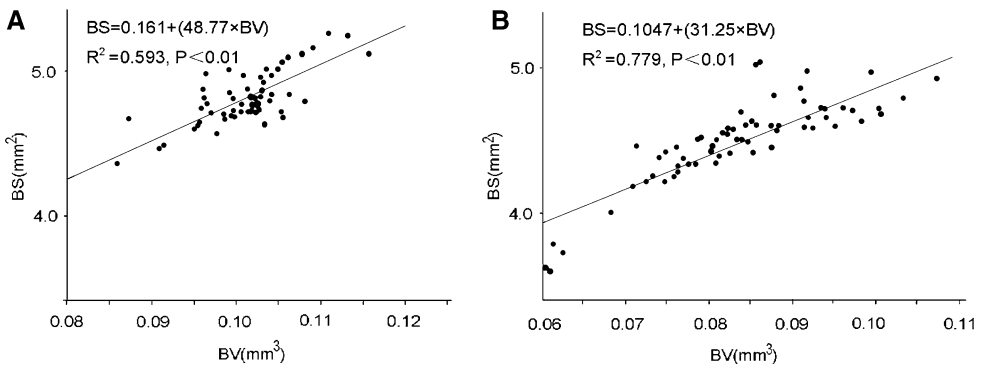

Fig. 6 Linear relationship between BV and BS in the control group (**a**) and the experimental group (**b**), assessed by micro-CT. The evaluated inclination was 31.25 in the experimental group and 48.77 in the control group. The effect, a decrease in BS accompanied by a decrease in BV, is less distinctive in the particle-treated group and attributed to irregular interblock osteolysis

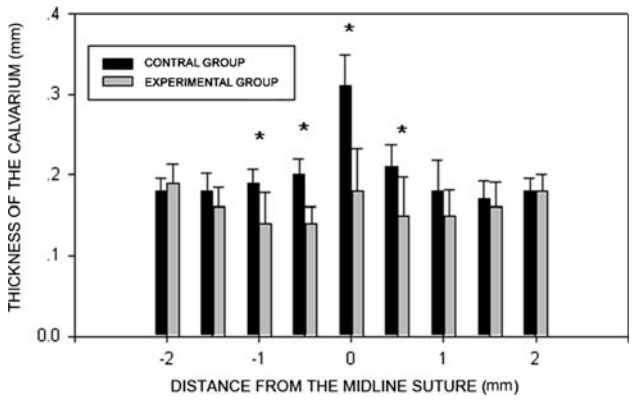

Fig. 7 Comparison of calvarial thickness in the control group (group 1) and in the experimental group (group 2). The histogram illustrates the irregular distribution of osteolysis seen in the coronal section by histological examination. Significant changes in calvarial thickness occurred close to the midline suture and not at the edge of calvarial specimens. $*P < 0.05$

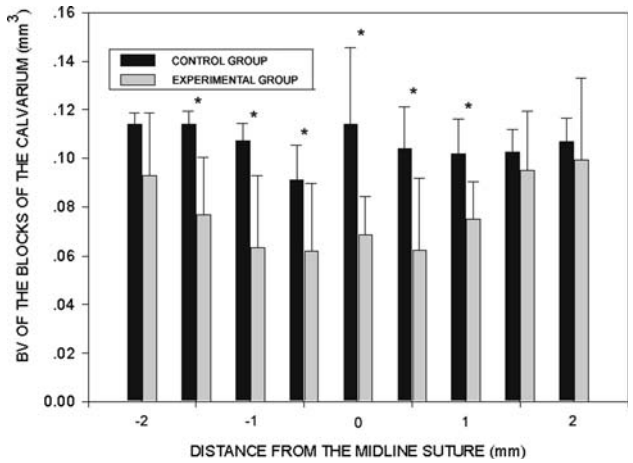

Fig. 8 Comparison of BV in the control group (group 1) and the experimental group (group 2). The histogram illustrates the irregular distribution of osteolysis seen in the coronal section by micro-CT. A significant difference in bone loss between the particle-treated group and the control group was found at a distance of 1.5 mm from the midline suture but not found via histomorphometric analysis (shown in Fig. 7). $*P < 0.05$

potential pathways for particle disease and accumulation via micro-CT in such an animal model, resulting in the development of implants well fixed to bone.

Furthermore, research on the distribution of osteopenia led us to focus on another unknown factor. In other current studies by our group [12, 13] we confirmed by means of micro-CT that mice which were null for the *Tac1* gene and α-CGRP knockout mice did not show significant particle-induced osteolysis. This finding was attributed to lack of substance P and α -CGRP. In this study micro-CT examination detected one animal in the particle-treated group which, in contrast to the other animals, showed an even and not irregular distribution of osteolytic lesions. This abnormal phenomenon, which might otherwise not have been revealed, encourages us to investigate in greater detail other unknown factors related to osteolysis.

In conclusion, the main advantages of micro-CT technology for evaluation of particle-induced osteolysis include (1) a fully automated means to quantify bone destruction within the entire specimen or ROI chosen, leading to more objective and faster results, and (2) 3D construction based on numerous slices with a section-to-section distance of less than 20 μm, which allows detection of even small changes.

Acknowledgements The study was supported by Biomaterialien NRW/Ministerium für Forschung und Wissenschaft. The authors thank Kaye Schreyer for editorial assistance with the manuscript and Priv. Doz. Dr. med. Frank Henschke for preparing the histology.

References

1. Silva MJ, Sandell LJ (2002) What's new in orthopaedic research. J Bone Joint Surg Am 84:1490–1496
2. Willert HG, Bertram H, Buchhorn GH (1990) Osteolysis in all-oarthroplasty of the hip. The role of ultra-high molecular weight polyethylene wear particles. Clin Orthop 258:95–107
3. Shanbhag AS, Hasselman CT, Rubash HE (1997) The John Charnley Award. Inhibition of wear debris mediated osteolysis in a canine total hip arthroplasty model. Clin Orthop 344:33–43
4. Merkel KD, Erdmann JM, McHugh KP, Abu-Amer Y, Ross FP, Teitelbaum SL (1999) Tumor necrosis factor α mediates orthopedic implant osteolysis. Am J Pathol 154:203–210
5. Schwarz EM, Benz EB, Lu AP, Goater JJ, Mollano AV, Rosier RN, Puzas JE, O'Keefe RJ (2000) Quantitative small animal surrogate to evaluate drug efficacy in preventing wear debris-induced osteolysis. J Orthop Res 18:849–855
6. Von Knoch M, Sprecher C, Barden B, Saxler G, Loer F, Wimmer M (2004) Grösse und Form kommerziell erhältlicher Polyethylenpartikel für in vitro und in vivo Versuche. Z Orthop 142:366–370
7. Child LM, Goater JJ, O'Keefe RJ, Schwarz EM (2001) Effect of anti-tumor necrosis factor-alpha gene on wear debris-induced osteolysis. J Bone Joint Surg Am 83:1789–1797
8. Taki N, Tatro JM, Lower R, Goldberg VM, Greenfield EM (2007) Comparison of the roles of IL-1, IL-6, and TNF-α in cell culture and murine models of aseptic loosening. Bone 40:1276–1283
9. Von Knoch M, Wedemeyer C, Pingsmann A, Von Knoch F, Hilken G, Sprecher C, Henschke F, Barden B, Löer F (2005) A single dose of zoledronic acid markedly decreases particle-induced bone resorption. Biomaterials 26:1803–1808
10. Wedemeyer C, Von Knoch F, Pingsmann A, Hilken G, Sprecher C, Saxler G, Henschke F, Löer F, Von Knoch M (2005) Stimulation of bone formation by zoledronic acid in particle-induced osteolysis. Biomaterials 26:3719–3725
11. Schwarz EM, Lu AP, Goater JJ, Benz EB, Kollias G, Rosier RN, Puzas JE, O'Keefe RJ (2000) Tumor necrosis factor-alpha/nuclear transcription factor-kappaB signaling in periprosthetic osteolysis. J Orthop Res 18:472–480
12. Wedemeyer C, Neuerburg C, Pfeiffer A, Heckelei A, Von Knoch F, Hilken G, Brankamp J, Henschke F, Von Knoch M, Loer F, Saxler G (2007) Polyethylene particle-induced bone resorption in substance P deficient mice. Calcif Tissue Int 80:268–274

13. Wedemeyer C, Neuerburg C, Pfeiffer A, Bylski D, Heckelei A, von Knoch F, Hilken G, Schinke T, Gosheger G, von Knoch M, Löer F, Saxler G (2007) Polyethylene particle induced bone resorption in alpha-calcitonin gene related peptide deficient mice. J Bone Miner Res 22:1011–1019
14. Feldkamp LA, Davis LC, Kress JW (1984) Practical cone-beam algorithm. J Opt Soc Am 1:612–619
15. Zhao S, Yu H, Wang G (2005) A unified framework for exact cone-beam reconstruction formulas. Med Phys 32:1712–1721
16. Perilli E, Baruffaldi F (2003) Proposal for shared collections of X-ray micro CT datasets of bone specimens. International Conference of Computional Bioengineering, Zaragoza, Spain
17. Parfitt AM (1988) Bone histomorphometry: proposed system for standardization of nomenclature, symbols, and units. Calcif Tissue Int 42:284–286
18. Sinha RK, Shanbhag AS, Maloney WJ, Hasselman CT, Rubash HE (1998) Osteolysis: cause and effect. Instr Course Lect 47:307–320
19. Willert HG, Semlitsch M (1977) Reactions of the articular capsule to wear products of artificial joint prostheses. J Biomed Mater Res 11:157–164
20. Kobayashi A, Freeman MAR, Bonfield W, Kadoya Y, Yamac T, Al-Saffar N, Scott G, Revell PA (1997) Number of polyethylene particles and osteolysis in total joint replacements. J Bone Joint Surg Br 79:844–848
21. Schuh A, Thomas P, Holzwarth U, Zeiler G (2004) Bilateral localized osteolysis after cemented total hip replacement. Orthopade 33:727–732
22. Park JS, Ryu KN, Hong HP, Park YK, Chun YS, Yoo MC (2004) Focal osteolysis in total hip replacement: CT findings. Skeletal Radiol 33:632–640
23. Uchiyama T, Tanizawa T, Muramatsu H, Endo N, Takahashi HE, Hara T (1997) A morphometric comparison of trabecular structure of human ileum between micro computed tomography and conventional histomorphometry. Calcif Tissue Int 61:493–498
24. Sran MM, Boyd SK, Cooper DM, Khan KM, Zernicke RF, Oxland TR (2007) Regional trabecular morphology assessed by micro-CT is correlated with failure of aged thoracic vertebrae under a posteroanterior load and may determine the site of fracture. Bone 40:751–757
25. Kinney JH, Lane NE, Haupt DL (1995) In vivo, three-dimensional microscopy of trabecular bone. J Bone Miner Res 10:264–270
26. Ruegsegger P, Koller B, Muller R (1996) A microtomographic system for the nondestructive evaluation of bone architecture. Calcif Tissue Int 58:24–29
27. Mitton D, Cendre E, Roux JP, Arlot ME, Peix G, Rumelhart C, Babot D, Meunier PJ (1998) Mechanical properties of ewe vertebral cancellous bone compared with histomorphometry and high-resolution computed tomography parameters. Bone 22:651–658
28. Yang SY, Yu H, Gong W, Wu B, Mayton L, Costello R, Wooley PH (2007) Murine model of prosthesis failure for the long-term study of aseptic loosening. J Orthop Res 25:603–611
29. Manley MT, Capello WN, D'Antonio JA, Edidin AA, Geesink RG (1998) Fixation of acetabular cups without cement in total hip arthroplasty: a comparison of three different implant surfaces at a minimum duration of follow-up of five years. J Bone Joint Surg Am 80:1175–1185
30. Capello WN, D'Antonio JA, Feinberg JR, Manley MT (1997) Hydroxyapatite-coated total hip femoral components in patients less than fifty years old: clinical and radiographic results after five to eight years of follow up. J Bone Joint Surg Am 79:1023–1029